Julia D. Wulfkuhle[1]
Joy A. Aquino[1]
Valerie S. Calvert[2]
David A. Fishman[3]
George Coukos[4]
Lance A. Liotta[1]
Emanuel F. Petricoin III[2]

[1]National Cancer Institute, Bethesda, MD, USA
[2]Food and Drug Administration, Bethesda, MD, USA
[3]Northwestern University Medical School, Chicago, IL, USA
[4]University of Pennsylvania, Philadelphia, PA, USA

Signal pathway profiling of ovarian cancer from human tissue specimens using reverse-phase protein microarrays

Defects in cell signaling pathways play a central role in cancer cell growth, survival, invasion and metastasis. An important goal of proteomics is to characterize and develop "circuit maps" of these signaling pathways in normal and diseased cells. We have used reverse-phase protein array technology coupled with laser capture microdissection and phospho-specific antibodies to examine the activation status of several key molecular "gates" involved in cell survival and proliferation signaling in human ovarian tumor tissue. The levels of activated extracellular-regulated kinase (ERK1/2) varied considerably in tumors of the same histotype, but no significant differences between histotypes were observed. Advanced stage tumors had slightly higher levels of phosphorylated ERK1/2 compared to early stage tumors. The activation status of Akt and glycogen synthase kinase 3β, key proteins and indicators of the state of the phosphatidylinositol 3-kinase/Akt pro-survival pathway also showed more variation within each histotype than between the histoypes studied. Our results demonstrate the utility of reverse phase protein microarrays for the multiplexed analysis of signal transduction from discreet cell populations of cells procured directly from human ovarian tumor specimens and suggest that patterns in signal pathway activation in ovarian tumors may be patient-specific rather than type or stage specific.

Keywords: Ovarian cancer / Protein microarrays / Signal transduction profiling PRO 0591

1 Introduction

An important goal of proteomics is to characterize and develop "circuit maps" of cellular signaling pathways in normal and diseased cells. Defective, hyperactive or dominating signal pathways may drive cancer growth, survival, invasion and metastasis [1]. Mapping the information flow through signaling pathways in normal and cancer cells may serve as a means to identify key alterations that occur during tumor progression and provide targets for rational, molecular-targeted drug design. Ovarian cancer is an example of a disease that could benefit greatly from more effective diagnosis and treatment. The majority of ovarian cancers are diagnosed at advanced stages and current treatment modalities do not provide significant hope for curing the disease. Altered expression or function of a number of kinases and phosphatases have been detected and are thought to participate in the development and progression of ovarian cancer. For example, the phosphatidylinositol 3-kinase (PI3K) pathway, associated with cell survival, is activated in a significant number of ovarian cancers and is thought to play an important role in the growth and invasion of tumors [2–4]. Genes encoding subunits of PI3K and its downstream target, Akt2, are amplified in primary ovarian tumors and overexpression of the Akt2 kinase is associated with aggressive, advanced stage cancers [5]. Mutations and down-regulation of the phosphatase/tensin homologue phosphatase have been observed in endometrioid carcinomas [6]. Alterations in mitogenic signaling pathways such as the mitogen-activated protein kinase (MAPK) pathway have also been examined in the context of ovarian carcinogenesis, particularly in the context of growth factor-related signaling. Overexpression of the Her2/Neu receptor is observed in 25–30% of ovarian cancers and is associated with poor prognosis [7]. In the past, efforts to elucidate the activation of signaling pathway events have relied mainly on either gene microarray/gene-based analysis and bioinformatic tools to help infer coordinate upstream signaling events or 2-D PAGE coupled with phosphorylation detection by immunoblotting [8–12]. Unfortunately, coordinate gene transcription profiling cannot accurately reflect post-translational modifications such

Correspondence: Dr. Julia D. Wulfkuhle, Center for Cancer Research, National Cancer Institute, Building 29A/Room 2B20, 8800 Rockville Pike, Bethesda, MD 20892, USA
E-mail: wulfkuhle@cber.fda.gov
Fax: +1-301-480-5005

Abbreviations: ERK, extracellular signal-regulated kinase; **GSK**, glycogen synthase kinase; **MAPK**, mitogen-activated protein kinase; **PI3K**, phosphatidylinositol 3-kinase

as protein phosphorylation that are the drivers of the cellular signaling processes. To understand the state of cellular signaling, new technologies that can characterize and directly monitor the activity and protein phosphorylation of various signaling pathways in small quantities of tumor tissue would be beneficial for both the identification of important targets for therapeutics and assessing the efficacy of these therapies. Reverse-phase protein microarrays represent a technology uniquely suited to screening a broad range of pathway targets in large numbers of tumors simultaneously in a high-throughput manner [13, 14]. Reverse-phase arrays are amenable for analysis of biopsy material and involve spotting nanoliter quantities of cellular lysates onto immobilized supports to allow for probing with specific antibodies. In this study, we used reverse-phase protein microarray technology to profile the activation state of key molecules involved in pro-survival and mitogenic signaling in microdissected ovarian tumor cells. We demonstrate that reverse-phase protein arrays provide an effective, high-throughput means to assess a large number of phosphospecific endpoints in human ovarian tumors. Our data suggest that levels of phosphorylated extracellular-regulated kinase (ERK1/2), activated Akt or GSK3b do not vary significantly with tumor histotype or disease stage and support the idea of that pathway activation profiles in ovarian tumors may be patient-specific.

2 Materials and methods

2.1 Tissue samples

Frozen ovarian tumor tissues were collected at the Abramson Family Cancer Research Institute at the University of Pennsylvania (Philadelphia, PA, USA) and the National Ovarian Cancer Early Detection Program clinic at Northwestern University Hospital (Chicago, IL, USA). The tissues were anonymized and approved for use by the National Cancer Institute Office of Human Subjects Research (Bethesda, MD, USA). The histopathology of each case was confirmed by a pathologist before use in these studies.

2.2 Tissue processing and microdissection

Eight μm frozen tissue sections were placed on uncoated glass slides and stored at −80°C prior to use. Immediately before dissection, the sections were thawed and fixed in 70% ethanol for 5 s, stained with hematoxylin for 8 s and dehydrated in 70, 95 and 100% ethanol for 1.5 min each followed by xylene for 2 min and then air-dried. The 70% ethanol and hematoxylin staining solutions were supplemented with Complete™ Mini protease inhibitor tablets (Roche Applied Science, Indianapolis, IN, USA). Ovarian tumor epithelial cells or other relevant cell populations were microdissected with a Pixcell II Laser Capture Microdissection system (Arcturus, Mountain View, CA, USA). Approximately 5000 laser capture microdissection shots (20 000–25 000 cells) were microdissected for each case and stored on microdissection caps at −80°C until lysed.

2.3 Cell lysis and cellular lysate arraying

Microdissected cells were lysed directly from the microdissection caps into 50 μL of lysis buffer containing a 1:1 mixture of 2x Tris-Glycine SDS Sample buffer (Invitrogen Life Technologies, Carlsbad, CA, USA) and Tissue Protein Extraction Reagent (Pierce, Rockford, IL, USA) plus 2.5% β-mercaptoethanol for 30 min at 75°C. The samples were boiled for 8 min, centrifuged briefly and stored at 4°C. A hydrogen peroxide-treated Jurkat cell lysate was used as a positive control for antibody staining. Immediately prior to arraying, lysates were loaded into a 384-well plate and serially diluted with lysis buffer into a five-point curve ranging from undiluted-1:16. Approximately 60 nL of each sample was spotted onto nitrocellulose-coated glass slides (Schleicher and Schuell Bioscience, Keene, NH, USA) with a GMSE 470 microarrayer (Affymetrix, Santa Clara, CA, USA). Slides were stored dessicated at −20°C. For estimation of total protein amounts, selected arrays were stained with Sypro Ruby Protein Blot Stain (Molecular Probes, Eugene, OR, USA) according to the manufacturer's instructions and visualized on a Fluorchem™ imaging system (Alpha Innotech, San Leandro, CA, USA). One day prior to antibody staining, the lysate arrays were treated with Reblot™ antibody stripping solution (Chemicon, Temecula, CA, USA) for 15 min at room temperature, washed two × five min in PBS, and then incubated overnight in blocking solution (1g I-block (Tropix, Bedford, MA, USA), 0.1% Tween-20 in 500 mL PBS) at 4°C with constant rocking.

2.4 Protein microarray staining

Blocked arrays were stained with antibodies on an automated slide stainer (Dako Cytomation, Carpinteria, CA, USA) using the Catalyzed Signal Amplification System kit according to the manufacturer's recommendation (CSA; Dako Cytomation). Briefly, endogenous biotin was blocked for 10 min using the biotin blocking kit (Dako Cytomation), followed by application of protein block for 5 min; primary antibodies were diluted in antibody diluent and incubated on slides for 30 min and biotinylated secondary antibodies were incubated for 15 min. Signal amplification involved incubation with a streptavidin-bio-

tin-peroxidase complex provided in the CSA kit for 15 min, and amplification reagent, (biotinyl-tyramide/hydrogen peroxide, streptavidin-peroxidase) for 15 min each. Development was completed using diaminobenzadine/hydrogen peroxide as the chromogen/substrate. Slides were allowed to air dry following development.

Primary and secondary antibodies and dilutions used in these studies were: rabbit anti-Akt 1:50 (Cell Signaling Technology, Beverly, MA, USA); rabbit anti-phosphoAkt S473 1:50 (Cell Signaling Technology); rabbit anti-phosphoAkt T308 1:50 (Cell Signaling Technology); rabbit anti-extracellular signal-regulated kinase (ERK)1/2 1:200 (Cell Signaling Technology); rabbit anti-phosphoERK1/2 T202/Y204 1:1000 (Cell Signaling Technology); rabbit anti-glycogen synthase kinase (GSK) 3β 1:500 (Chemicon, Temecula, CA, USA); rabbit anti-phospho GSK3 beta Y216 1:200 (Biosource International, Camarillo, CA, USA); biotinlyated goat anti-rabbit IgG (H+L) 1:5000 (Vector Laboratories, Burlingame, CA, USA); and biotinylated rabbit anti-mouse Ig 1:10 (Dako Cytomation).

2.5 Image analysis

Stained slides were scanned individually on a UMAX PowerLook III scanner (UMAX, Dallas, TX, USA) at 600 dpi and saved as TIF files in Photoshop 6.0 (Adobe, San Jose, CA, USA). The TIF images for antibody-stained slides and Sypro-stained slide images were analyzed with ImageQuant 5.2 (Molecular Dynamics, Sunnyvale, CA, USA) and Microsoft Excel 2000 software. For each antibody, the average pixel intensity value for the first point in each dilution curve was divided by the corresponding value from the Sypro-stained image of the slide to generate an intensity value normalized to the total protein present in each sample. The dilution curves were plotted to ensure that the dynamic range had not been saturated. Normalized intensity values were averaged with tumors of the same histotype and/or disease stage to generate histograms comparing changes in levels of phospho-specific endpoints between different tumor types or disease stages.

3 Results and discussion

3.1 Cases

A total of 40 cases encompassing major histotypes and stages of ovarian cancer were microdissected and arrayed as shown in Fig. 1A. The majority of cases (n = 31) were classified as endometrioid, serous papillary or poorly differentiated tumors. Certain less common histotypes (clear cell, mucinous, and mixed mesodermal) were represented by 2 cases each, and the array also included microdissected cells from a recurrent serous tumor, a benign fibrosarcoma, and a gastric signet ring tumor metastatic to the ovary. Due to their limited representation in this data set, these cases were omitted from further data analysis. The 31 cases included in the data analysis are indicated by asterisks in the right panel of Fig. 1A; the disease stage and histotype distribution for these cases are shown in Table 1.

Table 1. Distribution of tumors by histotype and disease stage

	Endometrioid	Serous papillary	Poorly differentiated	Total
Stage 1	2	2	2	6
Stage 2	0	1	1	2
Stage 3	4	7	9	20
Stage 4	2	1	0	3
Total	8	11	12	31

3.2 Protein microarray staining and analysis

We were interested in determining if ovarian tumors with various pathological and clinical parameters exhibit distinguishable patterns of signal pathway activation. Approximately 100 protein lysate arrays were printed from 40–50 μL of starting material for each case (Fig. 1A). These arrays were probed with antibodies against proteins representing key nodes in a wide variety of signaling cascades. All antibodies used in this study were first validated for specificity by Western blotting against microdissected tumor tissue lysates to ensure specificity (data not shown). Examples of typical staining results are illustrated in Fig. 1B and C. The majority of lysates on these arrays generally had robust staining for total ERK1/2 protein and total Akt (Fig. 1B and 1C, left panels). The anti-phospho ERK antibody also exhibited robust staining on the arrays and, while many lysates with intense staining for total ERK protein also had significant levels of phosphorylated ERK, there were cases where the level of activated ERK was significantly more or less intense (Fig. 1B, arrowheads, arrows).

Following staining, the arrays were scanned and analyzed in ImageQuant. Average pixel intensity values of the first spot in each dilution curve on the array were normalized to the intensity values obtained for total cellular protein staining in order to compare intensity values between tumor histotypes and disease stages. Through the analysis of the slope of the dilution curve, it was determined

A

Poorly Differentiated Stage 3	Clear Cell Stage 1	Serous Papillary Stage 3	Clear Cell Stage 3
Poorly Differentiated Stage 1	Poorly Differentiated Stage 3	Endometrioid Stage 3	Serous Papillary Stage 3
Endometrioid Stage 3	Endometrioid Stage 3	Poorly Differentiated Stage 3	Serous Papillary Stage 3
Recurrent Serous Tumor	Endometrioid Stage 1	Mucinous Stage 1	Serous Papillary Stage 2
Serous Papillary Stage 3	Serous Papillary Stage 3	Poorly Differentiated Stage 3	
Endometrioid Stage 4	Endometrioid Stage 3	Poorly Differentiated Stage 3	Serous Papillary Stage 3
Mixed Mesodermal Stage 3	Mucinous Stage 1	Poorly Differentiated Stage 3	Poorly Differentiated Stage 3
Poorly Differentiated Stage 3	Serous Papillary Stage 3	Serous Papillary Stage 1	Jurkat Cell Control
Serous Papillary Stage 1	Mixed Mesodermal Stage 3	Serous Papillary Stage 4	Poorly Differentiated Stage 3
Metastatic Signet Ring Tumor	Endometrioid Stage 1	Benign Fibrosarcoma	
Endometrioid Stage 4	Poorly Differentiated Stage 3	Poorly Differentiated Stage 1	

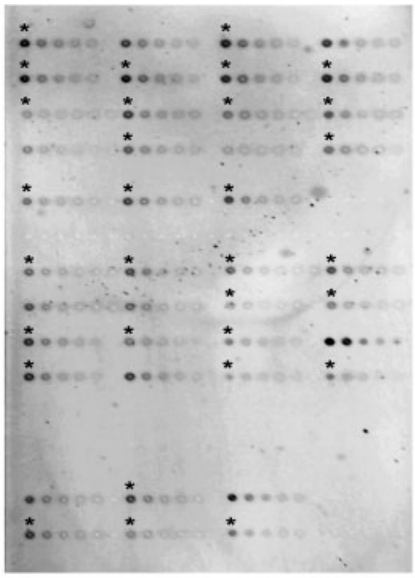

B

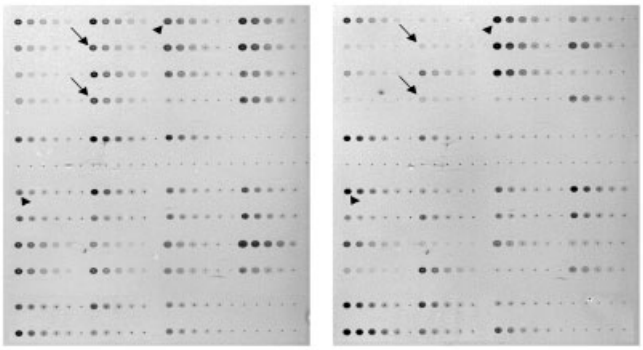

total ERK 1/2 pERK T202/Y204

C

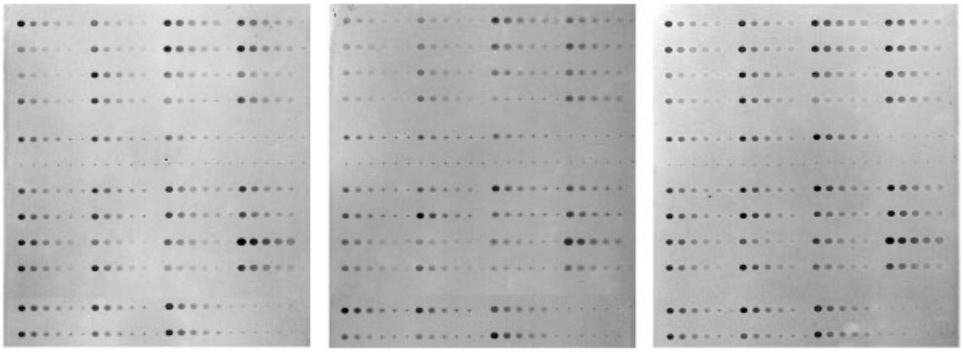

total Akt pAkt S473 pAkt T308

Figure 1. Examples of ovarian reverse-phase protein array layout and antibody staining. A, left panel: Diagram of ovarian array layout indicating tumor type and disease stage; right panel: Representative image of Sypro Ruby staining for total lysate protein on ovarian array. Asterisks indicate the position of the cases included in the data analysis. B: Reverse-phase arrays stained with ERK1/2 antibodies. Left panel: Image of total ERK1/2 antibody staining. Right panel: Image of phospho ERK1/2 T202/Y204 antibody staining. Arrows indicate examples of case in which staining for total protein is more intense than phosphoprotein staining; arrowheads indicate cases with more intense phosphoepitope staining *vs.* total protein staining. C: Examples of reverse-phase arrays stained with Akt antibodies. Left panel: total Akt antibody staining; middle panel: phospho Akt S473 antibody; right panel: phospho Akt T308 antibody.

that none of the points, including the most concentrated, were at saturation. Histograms comparing the average normalized intensity value of phosphoERK1/2 for each tumor type and stage are shown in Fig. 2. Average normalized values for total ERK1/2 did not vary significantly between different tumor types or disease stages (data not shown). The same was true for pERK1/2 when levels are compared by tumor type (Fig. 2A), but there was significant variation observed in the levels of staining within each tumor type. Comparison of the levels of phosphoERK between different disease stages revealed a modest increase in late stage tumors (Fig. 2B). Comparison of the levels of pERK protein between different stage tumors of the same histotype (Fig. 2C) showed that Stage 4 endometrioid tumors had higher average levels of the activated protein that any other type/stage category, however the small size of the study set precluded determination of statistical significance.

Deregulation of the Akt-dependent pro-survival pathway and MAPK cell proliferation pathways has been demonstrated in a number of solid tumors [15]. Previous studies have shown that the AKT2 gene is amplified in primary ovarian carcinomas and overexpression of the AKT2 kinase leads to increased invasion and metastasis [5, 16, 17]. Increased activity of the AKT1 kinase has also been observed in some ovarian tumors [18]. Because PI3K/AKT-dependent pathways have a potentially significant role in malignant transformation and tumor progression, we analyzed the level of activation of Akt as well as GSK3β in ovarian tumor tissues to determine if there were any correlations with tumor histotype or disease stage and the activation state of these pathways. Protein lysate arrays were probed with antibodies against total Akt, phosphoAkt S473 or phosphoAkt T308 (Fig. 1C). When normalized to total cellular protein, no significant differences in the average levels of Akt protein were observed when the data was grouped according to tumor histotype or disease stage (data not shown). Similarly, there was no significant difference seen in the level of either phosphorylated Akt S473 or T308 between tumor type and/or disease stage (Fig. 3). These data suggest that the levels of Akt activation are more likely to vary from patient to patient than between specific tumor histotypes.

4 Concluding remarks

As the drug discovery field places greater emphasis on the development of molecular-targeted therapeutics, this study underscores the need for the precise characterization of the activity status of pathways and targets of interest in individual tumors beyond levels of gene amplifica-

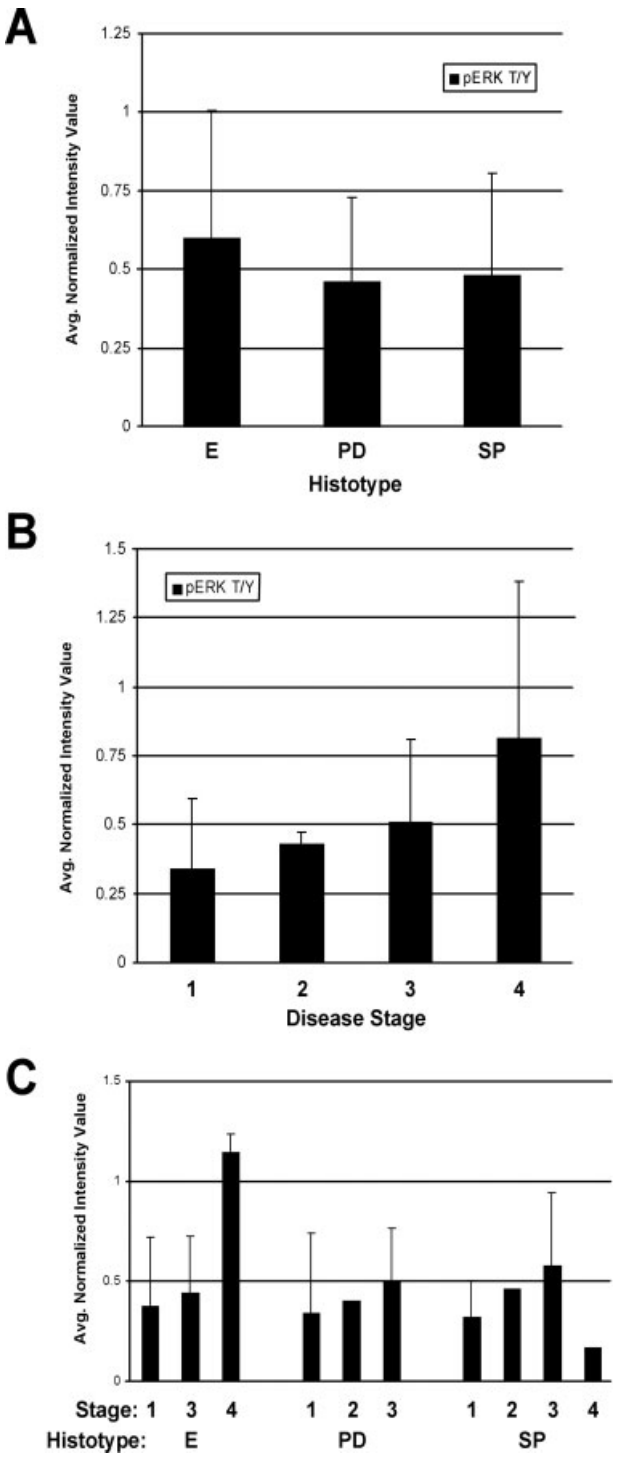

Figure 2. Comparisons of phosphoERK1/2 levels in ovarian tumors. Normalized intensity values for phosphoERK1/2 antibody staining were averaged among tumors of the same histotype (panel A) or disease stage (panel B). Panel C: histogram demonstrating the variation in phosphoERK levels between different disease stages within each tumor histotype. Error bars = SD from the mean; E = endometrioid; PD = poorly differentiated; SP = serous papillary.

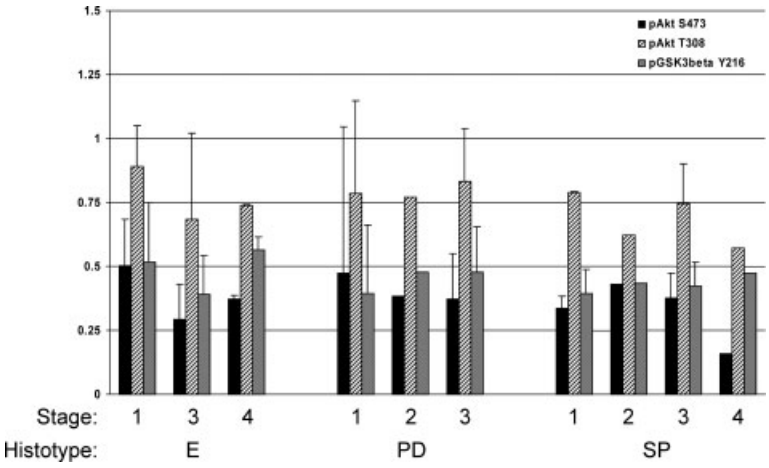

Figure 3. Comparisons of levels of phospho-specific endpoints in the PI3K/Akt signaling pathway. Average normalized values for pAkt S473 levels (black bars); pAkt T308 levels (striped bars), and pGSK3ß Y216 levels (hatched bars) are segregated by tumor type and disease stage. Error bars: SD from the mean. E = endometrioid; PD = poorly differentiated; SP = serous papillary.

tion and total protein expression. Gene microarray analysis alone cannot accurately recapitulate the states of these pathways and will be greatly complemented by proteomic analysis of the phosphorylation states of cellular circuitry. The detection of subtle changes in the activity of various signaling pathways in normal and tumor tissue in a patient is not only valuable scientifically for the study of disease progression, but will be essential for appropriate treatment selection and monitoring treatment efficacy in the future. This is especially so since the drug development pipeline is heavily skewed towards signal pathway modulators and kinase inhibitors. Reverse-phase protein microarray technology provides a means to detect, in a highly multiplexed way, these changes that are the direct targets for therapy. One observation from this study is that each ovarian cancer patient may have her own unique signal pathway activation portrait. In this case, effective targeting of the deranged pathways will need to be tailored to the specific derangements taking place. Future studies are now being planned to evaluate changes in the circuitry of ovarian cancer in relation to normal epithelial isolates, and to study changes in the epithelial and stromal compartments of high-risk patients. In the future, use of protein microarray technology that can specifically analyze the protein circuitry from biopsy material before, during and after therapy may provide a rational basis for the targeting of entire pathways using focused combinations of inhibitors selected for each patient.

Received May 23, 2003

5 References

[1] Liotta, L. A., Kohn, E. C., *Nature* 2001, *411*, 375–379.
[2] Hu, L., Zaloudek, C., Mills, G. B., Gray, J. *et al.*, *Clin Cancer Res.* 2000, *6*, 880–886.
[3] Shayesteh, L., Lu, Y., Kuo, W.-L., Baldocchi, R. *et al.*, *Nat. Genet.* 1999, *21*, 99–102.
[4] Philp, A. J., Campbell, I. G., Leet, C., Vincan, E. *et al.*, *Cancer Res.* 2001, *61*, 7426–7429.
[5] Bellacosa, A., De Feo, D., Godwin, A. K., Bell, D. W. *et al.*, *Int. J. Cancer* 1995, *64*, 280–285.
[6] Obata, K., Morland, S., Watson, R., Hitchcock, A. *et al.*, *Cancer Res.* 1998, *58*, 2095–2097.
[7] Slamon, D. J., Godolphin, W., Jones, L. A., Holt, J. A. *et al.*, *Science* 1989, *244*, 707–712.
[8] Lin, W. C., *Methods Mol. Biol.* 2003, *218*, 113–125.
[9] Omoto, Y., Hayashi, S., *Breast Cancer* 2002, *9*, 308–311.
[10] Perou, C. M., Sorlie, T., Eisen, M. B., van de Rijn, M. *et al.*, *Nature* 2000, *406*, 747–752.
[11] Ramaswamy, S., Perou, C. M., *Lancet* 2003, *361*, 1576–1577.
[12] Richards, J., Le Naour, F., Hanash, S., Beretta, L., *Ann. NY Acad. Sci.* 2002, *975*, 91–100.
[13] Paweletz, C. P., Charboneau, L., Bichsel, V. E., Simone, N. L. *et al.*, *Oncogene* 2001, *20*, 1981–1989.
[14] Liotta, L. A., Espina, V., Mehta, A. I., Calvert, V. *et al.*, *Cancer Cell.* 2003, *3*, 317–325.
[15] Vivanco, I., Sawyers, C. L., *Nat. Rev. Cancer* 2002, *2*, 489–501.
[16] Cheng, J. Q., Godwin, A. K., Bellacosa, A., Taguchi, T. *et al.*, *Proc. Natl. Acad. Sci. USA* 1992, *89*, 9267–9271.
[17] Arboleda, J. M., Lyons, J. F., Kabbinavar, F. F., Bray, M. R. *et al.*, *Cancer Res.* 2003, *63*, 196–206.
[18] Sun, M., Wang, G., Paciga, J. E., Feldman, R. I. *et al.*, *Am. J. Pathol.* 2001, *159*, 431–437.